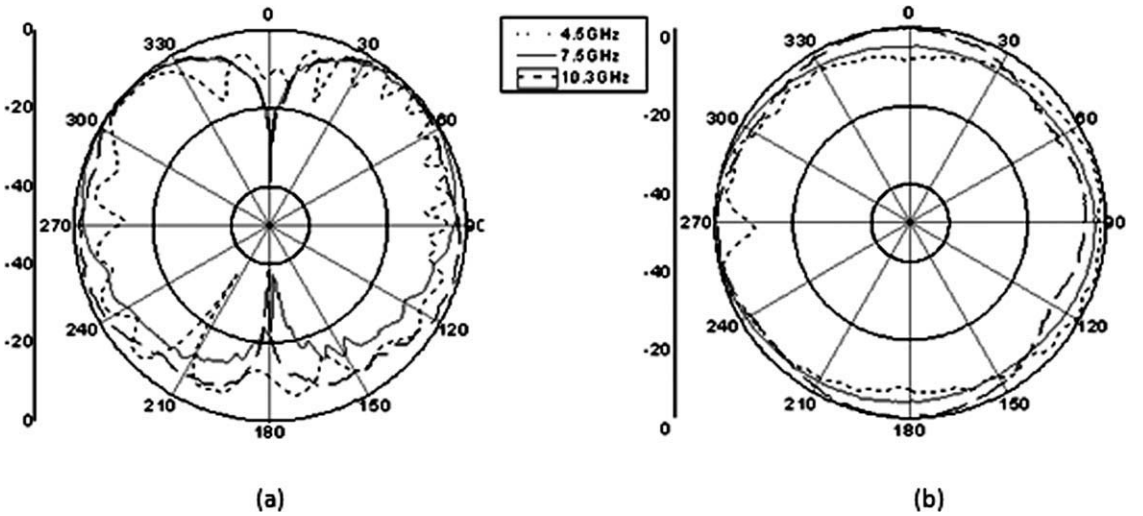

Figure 8 Measured radiation patterns on (a) *E*-plane and (b) *H*-plane for the proposed antenna

mm, L_{sh} = 8.2 mm, was fabricated and tested. The results in Figure 6 show the measurement results are similar to the simulation ones. The first notched band has a frequency deviation and the measured voltage standing wave ratio (VSWR) at higher frequencies are a little higher than the simulated ones. These are probably due to the losses offered by the SMA connector and un-matching among the antenna, SMA connector and vector network analyzer.

Simulated surface current distributions at 3.5 and 5.5 GHz are showed in Figure 7 to visualize each notched band. It is observed that the majority of the electric currents are concentrated around the L-shaped slot in the ground plane at 3.5 GHz, and around the eccentric ring and the stub with an arc structure at 5.5 GHz, resulting in a band-notched effect.

The measured *E*-plane and *H*-plane radiation patterns are shown in Figure 8. It can be seen that the proposed antenna has dipole-like radiation characteristics in *E*-plane and relatively omnidirectional radiation characteristics in *H*-plane.

4. CONCLUSIONS

A novel compact microstrip-fed antenna with a defected ground structure has been proposed. The simulated and measured results show the designed antenna covers the frequency from 3 to 32 GHz and has the dual band-notched characteristic to reject the interference with the 3.3–3.7 GHz WiMAX band and the 5.15–5.825 GHz WLAN band.

ACKNOWLEDGMENTS

This work was supported by the National Basic Research Program (973) under Grant 2009CB320204 and the National Natural Science Foundation under Grant 60821062 of China.

REFERENCES

1. S. Cheng, P. Hallbjorner, and A. Rydberg, Printed slot planar inverted cone antenna for ultrawideband applications, IEEE Antennas Wireless Propag Lett 7 (2008), 18–21.
2. M. Naser-Moghadasi, M. Koohestani, M. Golpour, and B.S. Virdee, Ultra-wideband square slot antenna with a novel diamond open-ended microstrip feed, Microwave Opt Technol Lett 51 (2009), 1075–1080.
3. C. Deng, Y.-J. Xie, and P. Li, CPW-fed planar printed monopole antenna with impedance bandwidth enhanced, IEEE Antennas Wireless Propag Lett 8 (2009), 1394–1397.
4. S.N. Khan, Z. Shuai, and S. He, Low profile and compact size coplanar UWB antenna working from 2.8 GHz to over 40 GHz, Microwave Opt Technol Lett 51 (2009), 408–411.
5. R. Gayathri, T.U. Jisney, D.D. Krishna, M. Gopikrishna, and C.K. Aanandan, Band-notched inverted-cone monopole antenna for compact UWB systems, Electron Lett 44 (2008), 1170–1171.
6. I.-T. Tang, D.-B. Lin, G.-H. Liou, and J.-H. Horng, Miniaturized 5.2 GHz notched UWB CPW-fed antenna using dual reverse split trapezoid slots, Microwave Opt Technol Lett 50 (2008), 652–655.
7. M. Ojaroudi, G. Ghanbari, N. Ojaroudi, and C. Ghobadi, Small square monopole antenna for UWB applications with variable frequency band-notch function, IEEE Antennas Wireless Propag Lett 8 (2009), 1061–1064.
8. M. Zhang, X. Zhou, J. Guo, and W. Yin, A novel ultrawideband planar antenna with dual band-notched performance, Microwave Opt Technol Lett 52 (2010), 90–92.

SIMPLE TWO-STRIP MONOPOLE WITH A PARASITIC SHORTED STRIP FOR INTERNAL EIGHT-BAND LTE/WWAN LAPTOP COMPUTER ANTENNA

Ting-Wei Kang and Kin-Lu Wong
Department of Electrical Engineering, National Sun Yat-Sen University, Kaohsiung, Taiwan 80424, Republic of China;
Corresponding author: kangtw@ema.ee.nsysu.edu.tw

Received 24 June 2010

ABSTRACT: *A dual-wideband internal antenna formed by a simple two-strip monopole (a longer strip and a shorter strip) and a parasitic shorted strip for eight-band long tern evolution/wireless wide area network operation (698–960/1710–2690 MHz) in the laptop computer is presented. The parasitic shorted strip is excited capacitively by the shorter strip of the two-strip monopole and contributes two resonant modes to the antenna, with one in the lower band and one in the upper band, thereby effectively widening the bandwidths of the antenna's two operating bands. Further, the parasitic strip short-circuited to the top shielding metal wall of the display ground in the laptop computer is configured such that its end section with the shorting point is positioned at the side edge of the antenna. This configuration allows the antenna to be placed closely to a nearby grounded plate, with very small effects on the performances of the antenna. This is an advantage for the proposed*

antenna in practical applications since the antenna requires a very small isolation distance at its side edge to nearby metal objects (such as a metal screw at the top shielding metal wall to fix the display ground to the casing of the laptop computer). Hence, in addition to the small antenna volume of 4 × 12 × 70 mm³ at the top shielding metal wall, compact integration of the proposed antenna along the shielding metal wall of the display ground can also be obtained. © 2011 Wiley Periodicals, Inc. Microwave Opt Technol Lett 53:706–712, 2011; View this article online at wileyonlinelibrary.com. DOI 10.1002/mop.25836

Key words: *monopole antennas; LTE antennas; WWAN antennas; internal laptop computer antennas; multiband antennas*

1. INTRODUCTION

To provide enhanced functionality in wireless internet access, it is required that the modern laptop computers be equipped with both the long tern evolution (LTE) [1] and wireless wide area network (WWAN) [2] operations. The LTE operation is recently introduced, which includes the LTE700 (698–878 MHz), LTE 2300 (2300–2400 MHz), and LTE2500 (2500–2690 MHz) bands and can provide much higher data rate than the WWAN operation in the 824–960 MHz (GSM850/900) and 1710–2170 MHz (GSM1800/1900/UMTS) bands. By combining both the LTE and WWAN operations, more seamless wireless internet access can also be obtained. Although many promising internal antennas for the penta-band WWAN operation (824–960/1710–2170 MHz) have been devised for the laptop computer applications [3–10], the internal antennas that can cover the eight-band LTE/WWAN operation (698–960/1710–2690 MHz) [11] are still very few. How to design the internal antennas with small size for application in the modern laptop computers is a design challenge.

In this article, we present a simple two-strip monopole with a parasitic shorted strip to provide two wide operating bands to respectively cover the LTE700/GSM850/900 (698–960 MHz) and GSM1800/1900/UMTS/LTE2300/2500 (1710–2690 MHz) as an internal eight-band LTE/WWAN laptop computer antenna. The simple two-strip monopole can lead to the generation of two operating bands for the proposed antenna. However, the obtained bandwidths of the two operating bands cannot cover the desired 698–960 and 1710–2690 MHz bands. By adding the parasitic shorted strip with a length close to a quarter-wavelength at about 750 MHz and capacitively excited by the shorter strip of the two-strip monopole, two additional resonant modes (one fundamental mode at about 750 MHz and one higher-order mode at about 1750 MHz) contributed by the parasitic shorted strip are generated to effectively enhance the bandwidths of the two operating bands of the proposed antenna. Hence, with a simple structure for the proposed antenna and a small antenna volume of 4 × 12 × 70 mm³ mounted at the top shielding metal wall of the display ground in the laptop computer, the eight-band LTE/WWAN operation is obtained.

Also, the parasitic shorted strip can be configured in the proposed antenna such that its end section with the shorting point is positioned at the side edge of the antenna. This configuration allows the antenna to be placed closely to a nearby grounded plate, with very small effects on the performances of the antenna. This is an advantage for the proposed antenna in practical applications since the antenna requires a very small isolation distance at its side edge to nearby metal objects (such as a metal screw at the top shielding metal wall to fix the display ground to the casing of the laptop computer) [12–17]. This can also lead to compact integration of the proposed antenna along the shielding metal wall of the display ground. Detailed operating

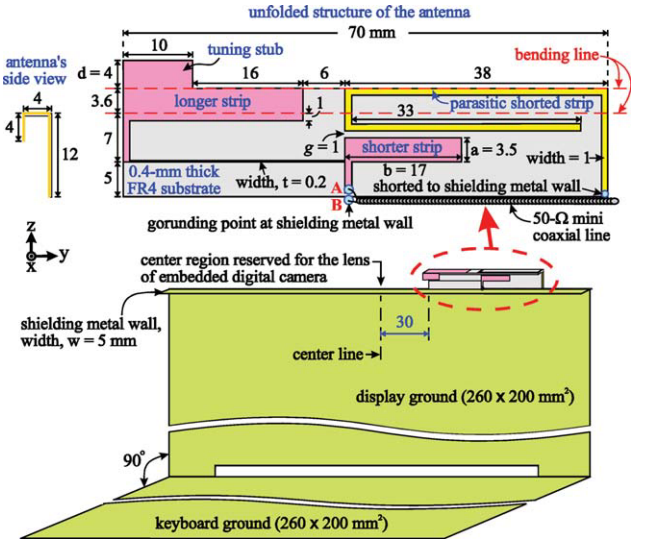

Figure 1 Geometry of the proposed two-strip monopole with a parasitic shorted strip for the eight-band internal LTE/WWAN laptop computer antenna. [Color figure can be viewed in the online issue, which is available at wileyonlinelibrary.com]

principle of the proposed antenna is described in the article. The antenna is also fabricated and tested, and obtained results are presented and analyzed.

2. DESIGN CONSIDERATIONS OF THE PROPOSED ANTENNA

Figure 1 shows the geometry of the proposed two-strip monopole with a parasitic shorted strip for the eight-band internal LTE/WWAN laptop computer antenna. The 13-inch laptop computer is modeled as a display ground and a keyboard ground [18], both of the same dimensions of 260 × 200 mm² and separated by an angle of 90°. At the top of the display ground, there is a shielding metal wall of width 5 mm and length 260 mm added to provide isolation between the internal antenna and the circuitry on the back side of the laptop display. Although the presence of the shielding metal wall usually results in some degrading effects on the impedance matching of the internal antenna, the proposed antenna with a small volume of 4 × 12 × 70 mm³ mounted at the top shielding metal wall can provide two wide operating bands to cover the desired eight-band operation. Also note that the proposed antenna is mounted along the top shielding metal wall with a spacing of 30 mm to the center line of the display ground. This arrangement is for the consideration that the center region is generally reserved for accommodating the lens of the embedded digital camera in the laptop computer.

Te proposed antenna has a simple structure of a two-strip monopole and a parasitic shorted strip. In the study, the antenna is mainly printed on a 0.4-mm thick FR4 substrate (relative permittivity 4.4 and loss tangent 0.024) which is bent into an inverted-L shape (12 mm in height and 4 mm in width) to be mounted at the top shielding metal wall. A small tuning stub made of a 0.2-mm thick copper plate and having a size of 4 × 10 mm² is connected to the longer strip of the two-strip monopole as shown in the figure to fine-adjust the impedance matching for frequencies over the antenna's lower band, which is formed by two resonant modes contributed respectively by the longer strip and the parasitic shorted strip. The longer strip provides a resonant path of about 68 mm. By further using a narrow front section of width 0.2 mm and length 32 mm for the longer strip,

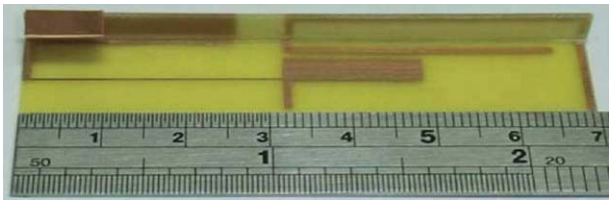

Figure 2 Photo of the fabricated antenna. [Color figure can be viewed in the online issue, which is available at wileyonlinelibrary.com]

the longer strip can generate a fundamental resonant mode at about 950 MHz and a higher-order resonant mode at about 2400 MHz for the proposed antenna. In this design, the narrow front section functions like a printed distributed inductor [19–26], which contributes additional inductance to compensate for the increased capacitance with a decrease in the resonant length. Thus, with a length of 68 mm only, a fundamental resonant mode at about 950 MHz can be generated by the longer strip of the two-strip monopole. Detailed effects of the width t of the narrow front section of the longer strip are analyzed in the next section.

On the other hand, the shorter strip with a length of about 25 mm can contribute a fundamental resonant mode at about 2850 MHz. Hence, with the two-strip monopole only, three resonant modes are provided to form two operating bands for the antenna. However, the bandwidths of the two operating bands are not wide enough for the desired eight-band operation.

To widen the bandwidths of the antenna, the parasitic shorted strip with a length of about 92 mm is added, which is short-circuited to the top shielding metal wall and capacitively excited through a 1-mm gap by the shorter strip of the two-strip monopole. In this case, the shorter strip is not only a radiator, but also a feeding strip for the parasitic shorted strip. The parasitic shorted strip can be successfully excited to generate a fundamental resonant mode at about 750 MHz and a higher-order resonant mode at about 1750 MHz. These two additional resonant modes combine the three modes contributed by the two-strip monopole to from two wide operating bands for the antenna to respectively cover the LTE700/GSM850/900 (698–960 MHz) and GSM1800/1900/UMTS/LTE2300/2500 (1710–2690 MHz) bands. Note that by varying the dimensions (width a and length b) of the shorter strip and the gap g between the shorter strip and the parasitic shorted strip, the capacitive excitation of the parasitic shorted strip can be adjusted such that good impedance matching of the excited resonant modes is obtained. Detailed effects of the parameters a, b, and g are presented in the next section. In addition, the parasitic shorted strip is also configured such that its end section with the shorting point is positioned at the side edge of the antenna, which allows the antenna to be placed closely to a nearby grounded plate, with very small effects on the performances of the antenna.

3. RESULTS AND DISCUSSION

The proposed antenna was fabricated and tested. Figure 2 shows the photo of the fabricated antenna. Results of the measured and simulated return loss for the fabricated antenna are shown in Figure 3. In the experiment, a 50-Ω mini coaxial line is used to feed the antenna, the same as in the practical laptop computer applications. The center conductor and outer grounding sheath of the coaxial line are respectively connected to point A (the front end of the shorter strip) and point B at the shielding metal wall, as shown in Figure 1. The simulated results are obtained

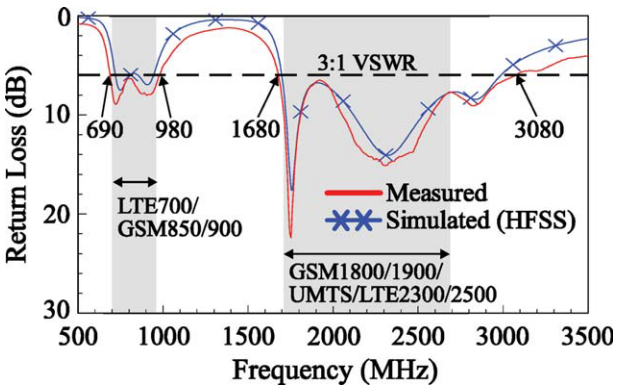

Figure 3 Measured and simulated return loss for the proposed antenna. [Color figure can be viewed in the online issue, which is available at wileyonlinelibrary.com]

using the Ansoft high frequency structure simulator [27], and good agreement between the measured and simulated results are obtained. Two wide operating bands have been obtained for the proposed antenna. The measured bandwidth, defined by 3:1 VSWR (6-dB return loss) which is widely used as the design specification for the internal WWAN antennas in practical mobile phone and laptop computer applications, is about 290 MHz (690–980 MHz) for the lower band and about 1400 MHz (1680–3080 MHz) for the upper band. The wide lower and upper bands cover the desired eight-band operation.

Figure 4 shows the simulated return loss for the proposed antenna, the case with the shorter strip only (Ref1), and the case with the shorter and longer strips only (Ref2). With the shorter strip only, a resonant mode in the desired upper band is generated. When the longer strip is added to form Ref2, two additional resonant modes are generated, with one mode at about 1 GHz (although the impedance matching is not good) and one mode at about 2400 MHz. The mode at about 2400 MHz also combines the one contributed by the shorter strip to widen the bandwidth of the antenna's upper band. Then, by further adding the parasitic shorted strip to form the proposed antenna, two additional resonant modes at about 750 and 1750 MHz are generated. The mode at 750 MHz combines the mode contributed by the longer strip to form a wide lower band for the antenna. Also, the mode at 1750 MHz combines the two modes contributed by the two-strip monopole to from the upper band. The

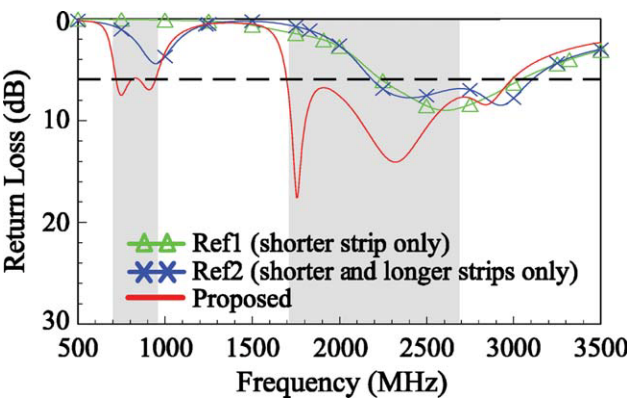

Figure 4 Simulated return loss for the proposed antenna, the case with the shorter strip only (Ref1), and the case with the shorter and longer strips only (Ref2). [Color figure can be viewed in the online issue, which is available at wileyonlinelibrary.com]

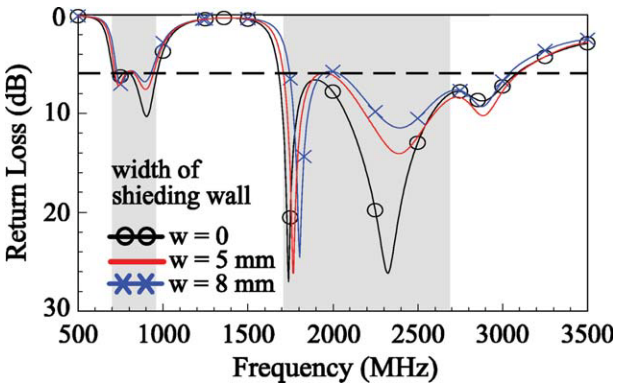

Figure 5 Simulated return loss for the proposed antenna as a function of the width w of the shielding metal wall. Other dimensions are the same as in Figure 1. [Color figure can be viewed in the online issue, which is available at wileyonlinelibrary.com]

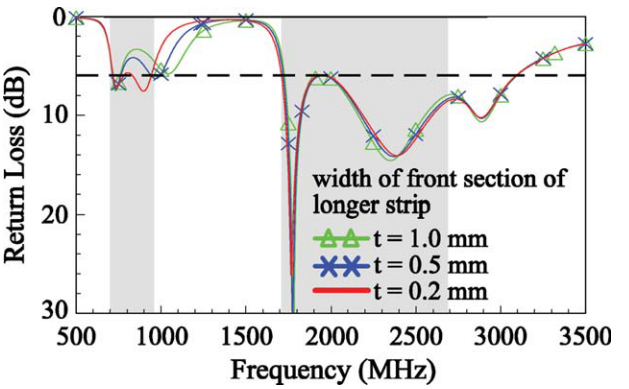

Figure 7 Simulated return loss for the proposed antenna as a function of the width t of the front section of the longer strip. Other dimensions are the same as in Figure 1. [Color figure can be viewed in the online issue, which is available at wileyonlinelibrary.com]

lower and upper bands therefore cover the desired eight-band operation.

Effects of the width w of the top shielding metal wall are studied in Figure 5. Results of the simulated return loss for the width w varied from 0 to 8 mm are shown. Other dimensions are the same as in Figure 1. Improved impedance matching for frequencies over both the lower and upper bands is seen for the case of $w = 0$ (the shielding metal wall not present). With the increase in the width w, the impedance matching also becomes degraded. The results suggest that the shielding metal wall should be taken into consideration in the internal antenna design for the laptop computer applications [28].

Figure 6 shows the simulated return loss for the proposed antenna with and without a nearby grounded metal plate. From the results, it is interesting to note that small effects are observed when a grounded metal plate (grounded to the shielding metal wall) is placed very close to the proposed antenna. In this study, the distance between the antenna (the end section of the parasitic shorted strip) and the grounded metal plate is selected to be 0.2 mm. As discussed in Section I, the grounded metal plate can be used to accommodate a metal screw at the top shielding metal wall to fix the display ground to the casing of the laptop computer.

Figure 7 shows the simulated return loss for the proposed antenna as a function of the width t of the front section of the longer strip. Results of the simulated return loss for the width t varied from 0.2 to 1.0 mm are shown. Large effects on the second mode or the mode contributed by the longer strip in the lower band are seen. When the width t is decreased, the second mode in the lower band is shifted to lower frequencies to combine the mode contributed by the parasitic shorted strip to form the desired lower band for the antenna. This effect is owing to the contributed inductance by the narrow front section to compensate for the increased capacitance of the decreased resonant length of the longer strip.

Effects of the tuning stub are studied in Figure 8. Results of the simulated return loss for the width d varied from 0 to 6 mm are shown in the figure. Improvements in the impedance matching of the second mode in the lower band and some shiftings of the second mode to lower frequencies are seen. This behaviour improves the impedance matching for frequencies in the desired lower band for the antenna. For other frequencies, small variations are seen. The results indicate that the tuning stub can be

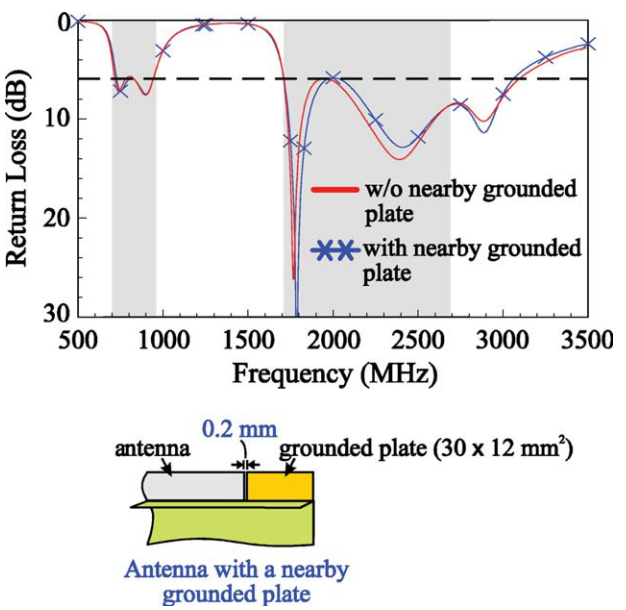

Figure 6 Simulated return loss for the proposed antenna with and without a nearby grounded metal plate. Other dimensions are the same as in Figure 1. [Color figure can be viewed in the online issue, which is available at wileyonlinelibrary.com]

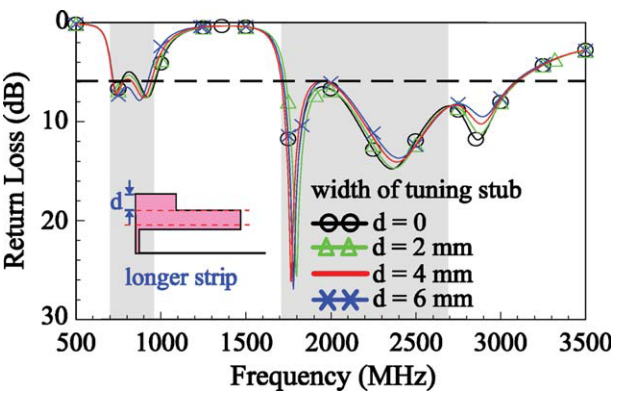

Figure 8 Simulated return loss for the proposed antenna as a function of the width d of the tuning stub in the longer strip. Other dimensions are the same as in Figure 1. [Color figure can be viewed in the online issue, which is available at wileyonlinelibrary.com]

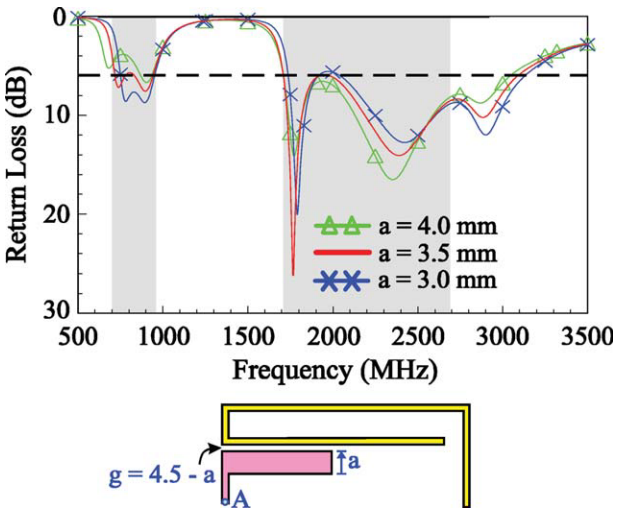

Figure 9 Simulated return loss for the proposed antenna as a function of the width *a* in the shorter strip. Other dimensions are the same as in Figure 1. [Color figure can be viewed in the online issue, which is available at wileyonlinelibrary.com]

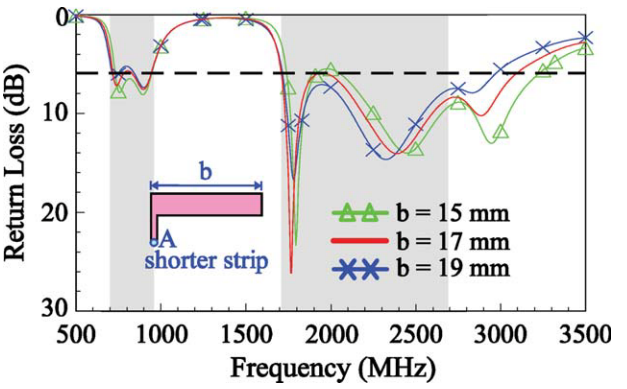

Figure 10 Simulated return loss for the proposed antenna as a function of the length *b* in the shorter strip. Other dimensions are the same as in Figure 1. [Color figure can be viewed in the online issue, which is available at wileyonlinelibrary.com]

used to effectively adjust the impedance matching of the antenna's lower band.

Figure 9 shows the simulated return loss as a function of the width *a* in the shorter strip. Results for the width *a* varied from 3.0 to 4.5 mm are shown. Note that when the width *a* varies, the gap *g* between the shorter strip and the parasitic shorted strip also varies as shown in the inset in the figure. Since the width *a* affects the capacitive coupling between the shorter strip and the parasitic shorted strip, large effects on the first mode of the lower band contributed the parasitic shorted strip are therefore observed. For the upper band, although there are some effects on the impedance matching of the three excited resonant modes, the obtained bandwidths can all cover the desired five-band operation of GSM1800/1900/UMTS/LTE2300/2500.

Effects of the length *b* in the shorter strip on the antenna performances are analyzed in Figure 10. Results for the length *b* varied from 15 to 19 mm are presented. Some effects on the first mode of the lower band, which is contributed by the parasitic shorted strip, are seen. The results indicate that the parameters *a*, *b*, and *g* are important for achieving improved impedance matching for frequencies over the lower band. For the upper band, although there are some variations in the three excited resonant modes in the band, the obtained bandwidths again can all cover the desired five-band operation in the 1710–2690 MHz band.

Measured radiation characteristics of the fabricated antenna are also studied. Figure 11 shows the measured radiation patterns at 830, 1940, and 2500 MHz for the antenna. At each

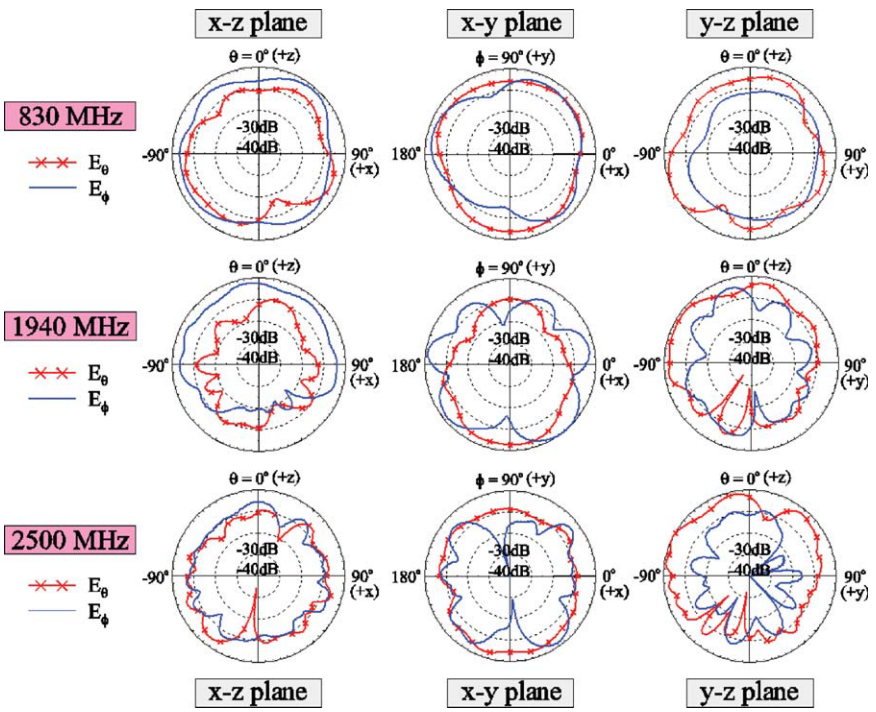

Figure 11 Measured radiation patterns at 830, 1940, and 2500 MHz for the fabricated antenna. [Color figure can be viewed in the online issue, which is available at wileyonlinelibrary.com]

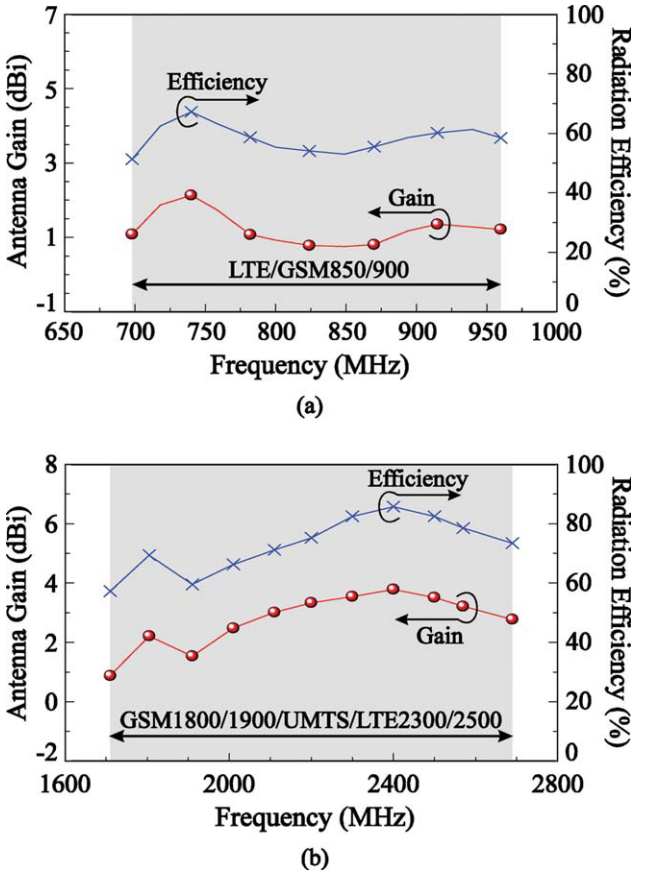

Figure 12 Measured radiation efficiency and antenna gain of the fabricated antenna. (a) The lower band. (b) The upper band. [Color figure can be viewed in the online issue, which is available at wileyonlinelibrary.com]

frequency, the radiation patterns in three principal planes are shown. Comparable E_θ and E_ϕ components are seen in the measured radiation patterns. Also, in the azimuthal plane (x-y plane), it is expected that the total power (E_θ and E_ϕ together) shows no nulls in all the ϕ angles. These radiation characteristics can lead to no communication nulls in practical applications.

Figure 12 shows the measured radiation efficiency and antenna gain of the fabricated antenna. The measured results show that the radiation efficiency is about 51–67% and 58–85% for the lower and upper bands, respectively. The measured antenna gain varies from about 0.8–2.0 dBi for the lower band and 1.0–3.8 dBi for the upper band. The measured radiation efficiency and antenna gain are acceptable for practical applications.

4. CONCLUSION

A promising internal laptop computer antenna for the eight-band LTE/WWAN operation has been proposed and studied. The antenna has a simple structure formed by a two-strip monopole and a parasitic shorted strip, and can be easily fabricated mainly by printing on a thin FR4 substrate at low cost. The parasitic shorted strip in the proposed design leads to widened bandwidths for both the lower and upper bands of the antenna. Successful excitation of the parasitic shorted strip has been obtained by using the shorter strip of the two-strip monopole as the coupling feed, which is also an efficient radiator to contribute a resonant mode for the antenna. The coupling feed in the proposed design is different from those of the traditional coupled-fed antennas [29–34] in which the coupling feed does not contribute resonant modes for the antenna. Also, with the parasitic shorted strip configured at the side edge of the antenna, effects of a nearby grounded metal object on the antenna performances can be greatly decreased. This can also lead to compact integration of the proposed antenna along the top shielding metal wall of the display ground in the laptop computer. Good radiation characteristics of the proposed antenna have also been observed. The measured radiation patterns with the E_θ and E_ϕ together show no nulls in all the ϕ angles in the azimuthal plane for the antenna. This can lead to no communication nulls in practical applications.

REFERENCES

1. S. Sesia, I. Toufik, and M. Baker (Eds.), LTE, The UMTS Long Term Evolution: From Theory to Practice, Wiley, New York, 2009.
2. K.L. Wong, Planar Antennas for Wireless Communications, Wiley, New York, 2003.
3. X. Wang, W. Chen, and Z. Feng, Multiband antenna with parasitic branches for laptop applications, Electron Lett 43 (2007), 1012–1013.
4. C.H. Chang and K.L. Wong, Internal coupled-fed shorted monopole antenna for GSM850/900/1800/1900/UMTS operation in the laptop computer, IEEE Trans Antennas Propagat 56 (2008), 3600–3604.
5. K.L. Wong and S.J. Liao, Uniplanar coupled-fed printed PIFA for WWAN operation in the laptop computer, Microwave Opt Technol Lett 51 (2009), 549–554.
6. K.L. Wong and L.C. Lee, Multiband printed monopole slot antenna for WWAN operation in the laptop computer, IEEE Trans Antennas Propagat 57 (2009), 324–330.
7. C. Zhang, S. Yang, S. El-Ghazaly, A.E. Fathy and V.K. Nair, A low-profile branched monopole laptop reconfigurable multiband antenna for wireless applications, IEEE Antennas Wireless Propagat Lett 8 (2009), 216–219.
8. K.L. Wong and F.H. Chu, Internal planar WWAN laptop computer antenna using monopole slot elements, Microwave Opt Technol Lett 51 (2009), 1274–1279.
9. C.W. Chiu, Y.J. Chi and S.M. Deng, An internal multiband antenna for WLAN and WWAN applications, Microwave Opt Technol Lett 51 (2009), 1803–1807.
10. C.T. Lee and K.L. Wong, Study of a uniplanar printed internal WWAN laptop computer antenna including user's hand effects, Microwave Opt Technol Lett 51 (2009), 2341–2346.
11. T.W. Kang and K.L. Wong, Internal printed loop/monopole combo antenna for LTE/GSM/UMTS operation in the laptop computer, Microwave Opt Technol Lett 52 (2010), 1673–1678.
12. K.L. Wong, C.H. Chang, and Y.C. Lin, Printed PIFA EM compatible with nearby conducting elements, IEEE Trans Antennas Propagat 55 (2007), 2919–2922.
13. K.L. Wong and C.H. Chang, Surface-mountable EMC monopole chip antenna for WLAN operation, IEEE Trans Antennas Propagat 54 (2006), 1100–1104.
14. K.L. Wong and C.H. Chang, WLAN chip antenna mountable above the system ground plane of a mobile device, IEEE Trans Antennas Propagat 53 (2005), 3496–3499.
15. C.M. Su, K.L. Wong, C.L. Tang, and S.H. Yeh, EMC internal patch antenna for UMTS operation in a mobile device, IEEE Trans Antennas Propagat 53 (2005), 3836–3839.
16. K.L. Wong, S.L. Chien, C.M. Su, and F.S. Chang, An internal planar mobile phone antenna with a vertical ground plane, Microwave Opt Technol Lett 47 (2005), 597–599.
17. K.L. Wong, S.W. Su, C.L. Tang, and S.H. Yeh, Internal shorted patch antenna for a UMTS folder-type mobile phone, IEEE Trans Antennas Propagat 53 (2005), 3391–3394.

18. T.W. Kang and K.L. Wong, Chip-inductor-embedded small-size printed strip monopole for WWAN operation in the mobile phone, Microwave Opt Technol Lett 51 (2009), 966–971.
19. J. Guterman, A.A. Moreira, C. Peixeiro, and Y. Rahmat-Samii, Wrapped microstrip antennas for laptop computers, IEEE Antennas Propagat Mag 51 (2009), 12–39.
20. J. Thaysen and K.B. Jakobsen, A size reduction technique for mobile phone PIFA antennas using lumped inductors, Microwave J 48 (2005), 114–126.
21. J. Carr, Antenna toolkit, 2nd ed., 111–112, Newnes, Oxford, 2001.
22. T.W. Kang and K.L. Wong, Chip-inductor-embedded small-size printed strip monopole for WWAN operation in the mobile phone, Microwave Opt Technol Lett 51 (2009), 966–971.
23. Y.W. Chi and K.L. Wong, Quarter-wavelength printed loop antenna with an internal printed matching circuit for GSM/DCS/PCS/UMTS operation in the mobile phone, IEEE Trans Antennas Propagat 57 (2009), 2541–2547.
24. C.H. Chang and K.L. Wong, Small-size printed monopole with a printed distributed inductor for penta-band WWAN mobile phone application, Microwave Opt Technol Lett 51 (2009), 2903–2908.
25. T.W. Kang and K.L. Wong, Very-small-size printed monopole with embedded chip inductor for 2.4/5.2/5.8 GHz WLAN laptop computer antenna, Microwave Opt Technol Lett 51 (2010), 171–177.
26. K.L. Wong and S.C. Chen, Printed single-strip monopole using a chip inductor for penta-band WWAN operation in the mobile phone, IEEE Trans Antennas Propagat 58 (2010), 1011–1014.
27. Ansoft Corporation HFSS. Available at http://www.ansoft.com/products/hf/hfss/.
28. S.Y. Lin, Multi-band folded planar monopole antennas for mobile handset, IEEE Trans Antennas Propagat 52 (2004), 1790–1794.
29. C.H. Chang and K.L. Wong, Printed λ/8-PIFA for penta-band WWAN operation in the mobile phone, IEEE Trans Antennas Propagat 57 (2009), 1373–1381.
30. C.H. Wu and K.L. Wong, Ultra-wideband PIFA with a capacitive feed for penta-band folder-type mobile phone antenna, IEEE Trans Antennas Propagat 57 (2009), 2461–2464.
31. K.L. Wong and C.H. Huang, Bandwidth-enhanced internal PIFA with a coupling feed for quad-band operation in the mobile phone, Microwave Opt Technol Lett 50 (2008), 683–687.
32. C.T. Lee and K.L. Wong, Uniplanar coupled-fed printed PIFA for WWAN/WLAN operation in the mobile phone, Microwave Opt Technol Lett 51 (2009), 1250–1257.
33. C.T. Lee and K.L. Wong, Uniplanar printed coupled-fed PIFA with a band-notching slit for WLAN/ WiMAX operation in the laptop computer, IEEE Trans Antennas Propagat 57 (2009), 1252–1258.
34. C.R. Rowell and R.D. Murch, A compact PIFA suitable for dual-frequency 900/1800-MHz operation, IEEE Trans Antennas Propagat 46 (1998), 596–598.

WIDEBAND COMPOSITE AMC SURFACES FOR RCS REDUCTION

Yunqi Fu, Youquan Li, and Naichang Yuan
College of Electrical Science and Engineering, National University of Defense Technology, Hunan 410073, China; Corresponding author: yunqifu@yahoo.com.cn

Received 24 June 2010

ABSTRACT: *A composite artificial magnetic conductor (AMC) surface is presented for wide band radar cross section (RCS) reduction. The composite surface consists of two kinds of AMC cells with different resonance frequencies. The phase difference between them can be tuned to be within a range close to ±π over a wide bandwidth. Therefore, the reflections from these two different AMC cells cancel each other. The basic principle was discussed and a sample was measured. The results show that a nearly 10 dB RCS reduction was achieved with a 32% bandwidth.* © 2011 Wiley Periodicals, Inc. Microwave Opt Technol Lett 53:712–715, 2011; View this article online at wileyonlinelibrary.com. DOI 10.1002/mop.25835

Key words: *artificial magnetic conductor (AMC); wideband; radar cross section (RCS); reduction*

1. INTRODUCTION

Mushroom-like electromagnetic bandgap (EBG) structures [1] exhibit zero reflection coefficient phase at the resonance frequency. Thus, the EBG surface can be regarded as artificial magnetic conductor (AMC). This property has been used to design thin radar absorbing materials. This is a modified design of the Salisbury screen [2]. The Salisbury screen consists of a lossy resistive sheet placed $\lambda/4$ above a perfectly electrical conducting (PEC) ground plane. This $\lambda/4$ height limitation makes the Salisbury screen very bulky at low frequencies. Engheta [3] presented an AMC-based design with the overall thickness considerably reduced. Further consideration focused on the bandwidth and angular stability [4, 5]. Alternatively, AMC surfaces loaded with lumped resistors joining the adjacent metal patches were considered and applied in antenna radar cross section (RCS) reduction [6–10].

Another way of using AMC surfaces to control the electromagnetic scattering from targets is based on shaping. The principle is to reflect the electromagnetic signals away from the direction of incoming waves. A composite surface of AMC and PEC cells was proposed in [9]. The RCS reduction ability of the composite surface was based on the cancellation of the reflection contributions from PEC and AMC parts. The PEC and the AMC cells were arranged to form a chessboard like configuration. In the absence of any lossy components, the energy is not absorbed, but scattered in offset directions.

It should be noted that a disadvantage of AMC-based RCS reduction materials is their narrow bandwidth. The above mentioned two applications strongly depend on the AMC characteristic and this varies dramatically with frequency. In this letter, we proposed a wideband low RCS surface design based on composite AMC structures. Similar but different to the configuration in [9], we adopted two AMC cells with different resonance frequencies. By choosing the resonance frequencies of these two AMC structures, the phase difference between them can be tuned to be close to 180° in a much wider frequency range. Thus, the reflection from these two AMC cells can cancel each other (meaning a wideband RCS reduction surface). The basic design principle is discussed for the chessboard like composite surface, and a sample was made and measured.

2. DESIGN PRINCIPLES

The geometry illustration of the proposed composite AMC surface is depicted in Figure 1. Two different square AMC surfaces are arranged in a chessboard configuration. Specifically, a unit cell consists of two square AMC1 surfaces and two square AMC2 surfaces. It can also be seen from the figure that each square AMC surface is a finite array of periodic metal patches and shorting vias. Of importance is that AMC1 and AMC2 have different resonance frequencies (different zero reflection coefficient phase frequencies).

The total reflected energy from the composite surface is a summation of the reflection from both AMC1 and AMC2 cells.